JOC The Journal of Organic Chemistry

Article

pubs.acs.org/joc

Recognition and Sensing of Biologically Relevant Anions in Alcohol and Mixed Alcohol–Aqueous Solutions Using Charge Neutral Cleft-Like Glycol-Derived Pyridyl–Amidothiourea Receptors

Rebecca M. Duke, Thomas McCabe, Wolfgang Schmitt, and Thorfinnur Gunnlaugsson*

School of Chemistry, Center for Synthesis and Chemical Biology, Trinity College Dublin, Dublin 2, Ireland

Supporting Information

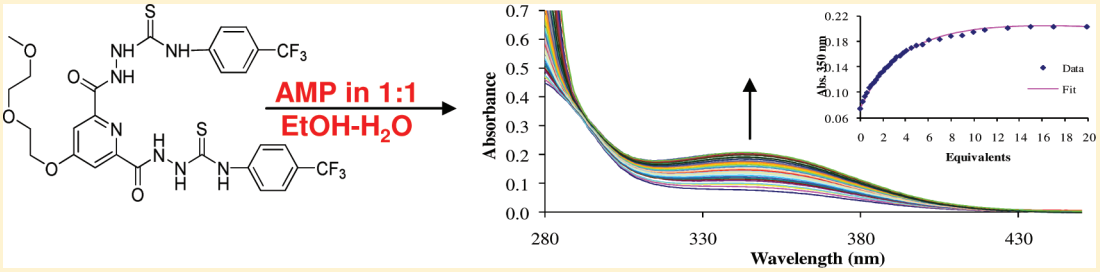

ABSTRACT: In this paper, the synthesis and the spectroscopic investigation of new colorimetric receptors for anions **3**–**6**, possessing a glycol chain at the 4-position of the pyridyl ring, and **1** and **2**, which lack such a chain, and the X-ray crystal structure of **2** is presented. Structures **3**–**6** are able to bind to anions in competitive media, such as alcohol or in a mixture of methanol and water, where the anion recognition gives rise to changes in the absorption spectra, which is red-shifted, in 1:1 or 1:2 (sensor/anion) stoichiometry. The anion recognition for **1** and **2** was also investigated in organic solvents and in a 4:1 mixture of DMSO/H_2O. The binding of **1** to anions such as acetate, phosphate, and fluoride was also evaluated using ^{1}H NMR in DMSO-d_6.

INTRODUCTION

The design and study of luminescent and colorimetric sensors for anions has become a very active area of research within the field of supramolecular chemistry.[1,2] While anions can be bound to positively charged receptors, the use of charge-neutral anion recognition moieties to achieve anion binding has been the focus of many publications in recent years.[3−5] Most of these examples have been designed for use in organic solution, where the anion recognition process occurs via hydrogen bonding. In contrast, only a few examples of such recognition/sensing using hydrogen bonding in more competitive aqueous media have been published.[5g] We have developed both colorimetric- and luminescent-based sensors for anions using urea- and thiourea-based sensors.[5,6] Recently, we have also developed such fluorescent sensors possessing amidourea or amidothiourea functionalities as anion receptors,[7] but these binding motifs have been shown, in particular by Jiang et al. and Gale et al., to give rise to strong interactions with anions such as acetate and phosphates.[8] We have also incorporated these into colorimetric sensors based on structures such as 1,8-naphthalimides,[1,9] calixarenes[10] and various aryl groups and investigated their ability to sense anions in organic solutions such as DMSO and CH_3CN.

With the aim of further exploring the use of these binding motifs for anion sensing, particularly in competitive aqueous media, we have now developed the pyridyl–dicarboxyl systems **3**–**6**, which possess a poly(ethylene glycol) chain at the 4-postions of the pyridyl ring, and compounds **1** and **2**,[11] which lack such a solubilizing group, Figure 1. Compounds **1**–**6** were also developed with the view of binding anions through a cooperative effect, where the pyridyl unit preorganized the two amidothiourea moieties into a cleftlike[12a] arrangement. When we commenced this study, compound **2** was first formed and studied, as we had experienced significant changes in the UV–vis absorption spectra of related systems. Because of this, a greater number of anions were tested for **2** than **1**. We were only able to study **2** in detail in DMSO and various other organic solvents as well as in a 4:1 mixture of DMSO/H_2O solution, while compound **1** was studied predominantly in DMSO and in a 4:1 mixture of DMSO/H_2O solution, with the view of evaluating the effect of the substituent on the amidothiourea moiety. Hence, these compounds function as model compounds in the present discussion. In this paper, we show that the incorporation of a polyethylene chain into the pyridyl moieties of **3** and **4** greatly increases their solubility in protic solvents, while such modification also facilitates the incorporation of two pyridyl clefts, **5** and **6**, into a single structure, which should enable the detection of anions such as organic phosphates. We also demonstrate that the anion recognition can either be through the mechanism of hydrogen bonding or via deprotonation, both of which give rise to changes in the absorption spectra of these compounds.

Received: November 17, 2011
Published: February 23, 2012

ACS Publications © 2012 American Chemical Society

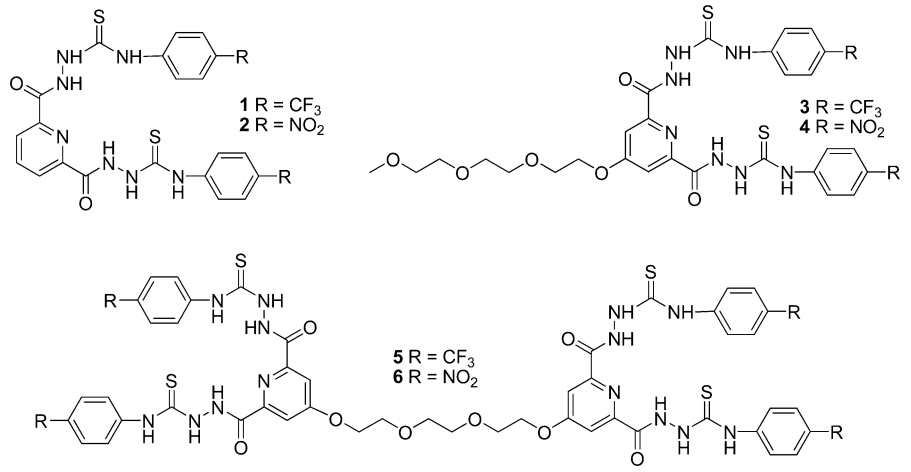

Figure 1. Structures **1**–**6** developed in this study.

Scheme 1[a]

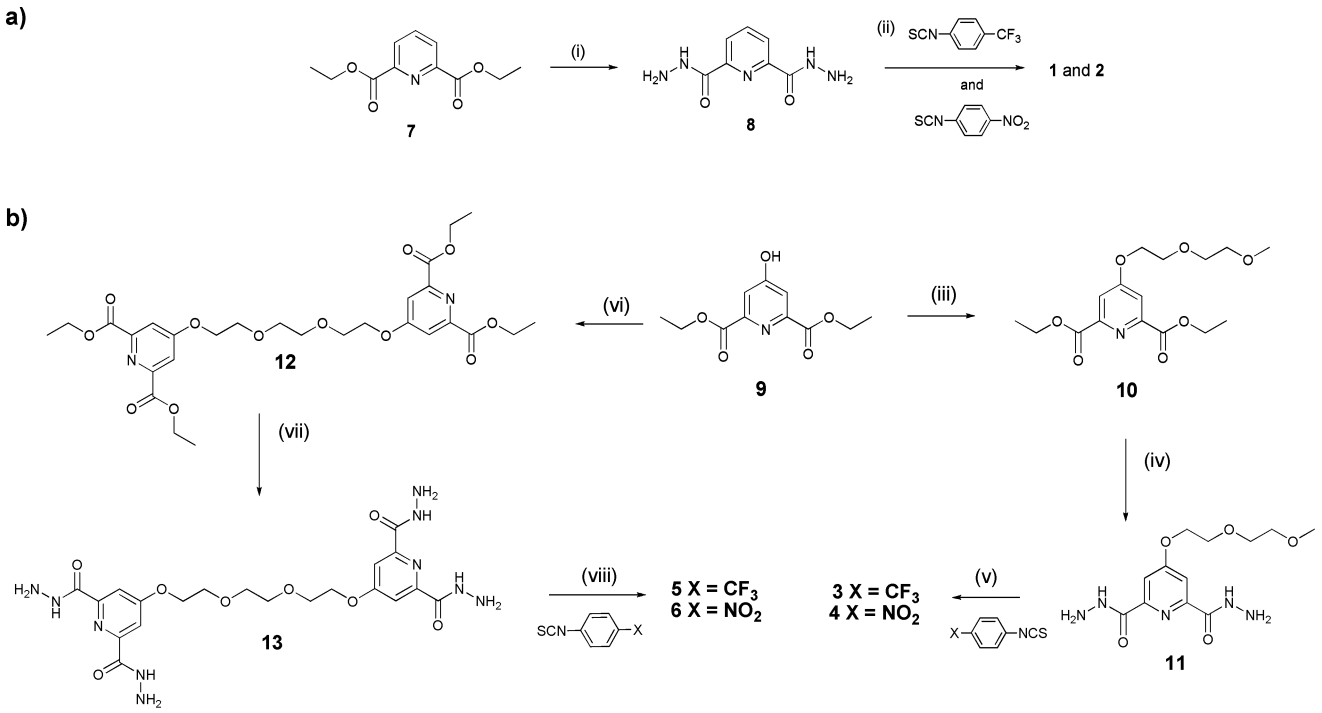

[a]Key: (a) (i) $N_2H_4{\cdot}H_2O$, MeOH, rt; (ii) CH_3CN, reflux, 16 h and either 4-trifluoromethylphenyl isothiocyanate or *p*-nitrophenyl isothiocyanate, giving **1** and **2**, respectively. (b) (iii) 1-Iodo-2-(2- methoxyethoxy)ethane, K_2CO_3, DMF, 80 °C, 16 h; (iv) $N_2H_4{\cdot}H_2O$, EtOH, reflux, 16 h; (v) 4-trifluoromethylphenyl isothiocyanate or *p*-nitrophenyl isothiocyanate, MeCN, reflux, 16 h, giving **3** and **4**, respectively; (vi) di(iodoethoxy)ethane, K_2CO_3, DMF, 80 °C, 16 h; (vii) $N_2H_4{\cdot}H_2O$, EtOH, reflux, 16 h; (viii) 4-trifluoromethylphenyl isothiocyanate or *p*-nitrophenyl isothiocyanate, MeCN, reflux, 16 h, giving **5** and **6**, respectively.

RESULTS AND DISCUSSION

Synthesis of 1–6 and X-ray Crystallographic Analysis of 2. The synthesis of **1** was achieved in a few linear steps as shown in Scheme 1a, where the commercially available 2,6-pyridinedicarboxylic acid was first converted to its corresponding diethyl ester **7**,[12a] followed by reacting it in refluxing MeOH with hydrazine monohydrate. This gave 2,6-pyridinedicarboxylic acid, dihydrazide **8**,[12b] which upon reaction with 4-trifluoromethylphenyl isothiocyanate in CH_3CN gave **1** as a white solid in 77% yield. Compound **2** was formed in a similar manner using 4-nitrophenyl isothiocyanate in 98% yield as a pale yellow solid. The ^{1}H NMR (600 MHz, DMSO-d_6) of both **1** and **2** showed the presence of two rotamers in solution. In the case of **2**, three broad resonances occurred at 11.30, 10.37, and 10.20 ppm, respectively, for the three N–H protons of the major isomer. These were assigned using various 2D NMR experiments and variable temperature NMR. In contrast, when the ^{1}H NMR of **2** was recorded in DMF-d_7 at room temperature only a single rotamer was observed.

The synthesis of **3**–**6** is shown in Scheme 1b and is based on the same synthetic strategy as for **1** and **2**, beginning with **9**, the diethyl ester of the commercially available chelidamic acid (formed by refluxing in EtOH in the presence of a catalytic amount of H_2SO_4),[13] which was placed in DMF in the presence of 1 equiv of K_2CO_3 and stirred at room temperature for 15

dx.doi.org/10.1021/jo202332h | J. Org. Chem. 2012, 77, 3115–3126

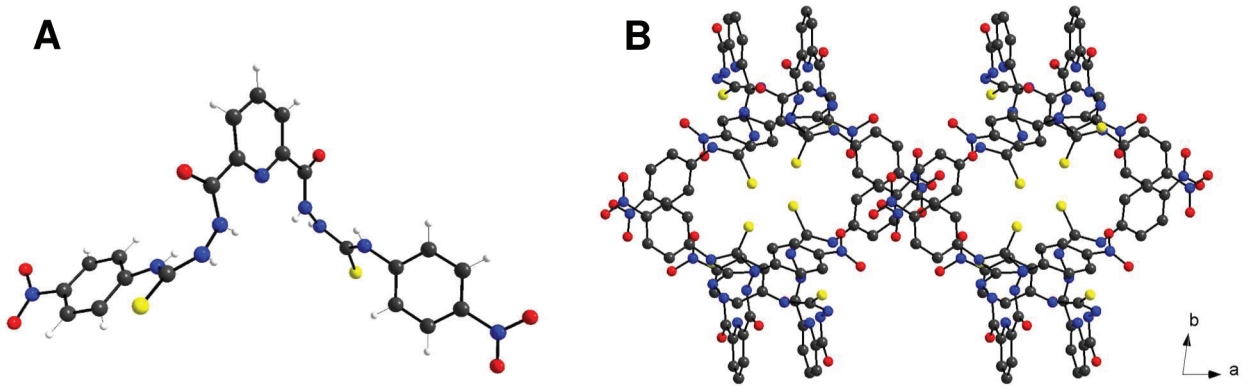

Figure 2. (A) X-ray crystal structure of **2**. Solvent molecules have been removed for clarity. (B) Packing of **2** when viewed down the crystallographic *c*-axis. Any solvent molecules and hydrogen atoms have been omitted for clarity.

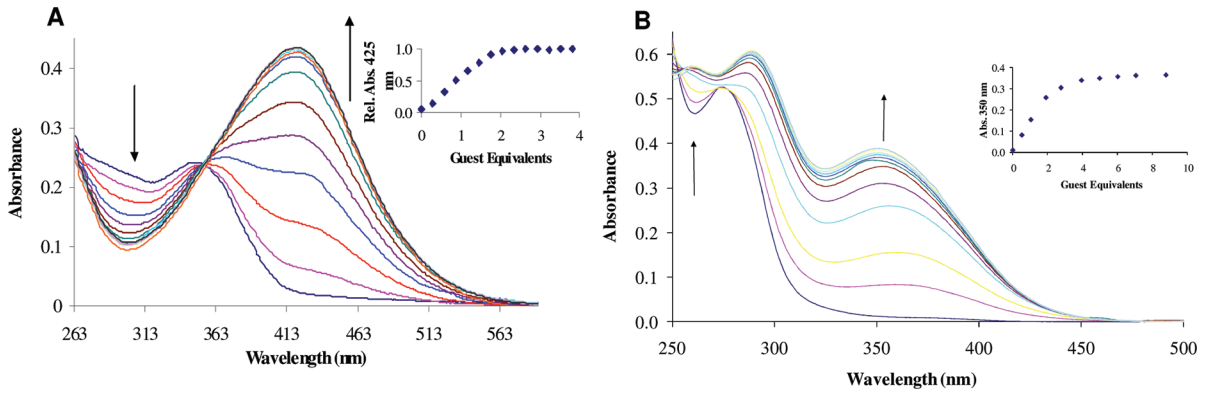

Figure 3. (A) Changes in the absorption spectra of **2** (1×10^{-5} M) upon addition of $H_2PO_4^-$ (0 → 5 equiv) in DMSO. Inset: Relative changes in the absorbance at 425 nm against equivalents of $H_2PO_4^-$. (B) Changes in the absorption spectrum of **1** (1.9×10^{-5} M) upon titration with AcO^- (0→9 equiv) in MeCN (with 1% DMSO). Inset: Changes at 360 nm.

min, after which 1-iodo-2-(2- methoxyethoxy)ethane[14] was added and the resulting solution heated at 80 °C for 16 h. After acidic workup, **10** was isolated as a yellow oil in 67% yield. Treatment of **10** with excess hydrazine in EtOH under reflux for 16 h resulted in the formation of **11** as a precipitate in 51% yield, which was reacted further under reflux with 2 equiv of either 4-trifluoromethylphenyl isothiocyanate or *p*-nitrophenyl isothiocyanate in MeCN, giving **3** and **4**, respectively, as off-white precipitates in 66% and 98% yields, respectively.

For the synthesis of **5** and **6**, the diester **9** was reacted with di(iodoethoxy)ethane in the presence of K_2CO_3 in DMF at 80 °C to give **12** as a yellow oil in 73% yield after recrystallization from EtOH. This intermediate was further reacted with hydrazine in EtOH to give the tetra hydrazide **13** in 81% yield as a white precipitate, which upon reaction with 4 equiv of 4-trifluoromethylphenyl isothiocyanate and *p*-nitrophenyl isothiocyanate gave **5** and **6** as pale yellow solids in 68% and 42% yields, respectively.

The compounds were fully characterized (see the Experimental Section). As an example, the ^{1}H NMR (see Figures S1−S6, Supporting Information, 400 MHz, DMSO-d_6 for **1**−**6**) of **3** showed the presence of the three sets of N−H protons, resonating at 11.25, 10.19, and 10.04 ppm for the amido and the two thiourea protons, respectively, while using HR MALDI MS gave an m/z peak for the $[M + H]^+$ ion at 720.1533. Recrystallization of sensors **3**−**6**, using a variety of solvents, generally resulted in the formation of poor quality crystals. However, in the case of **6**, crystals grown from a solution of EtOH−DMSO were found to be of satisfactory quality for X-ray crystallographic diffraction analysis.[15] The resulting structure, was, however, not of good enough quality for publication, but we were able to demonstrate the correct connectivity from the data obtained. We were, however, also able to grow crystals of **2** suitable for single-crystal X-ray crystallographic analysis[15] from a DMSO solution, the structure of which is shown in Figure 2A. The combination of H-bonding and $\pi-\pi$ stacking also gave rise to an elaborate 3D network that was perforated with ordered DMSO solvent-filled channels, Figure 2B. Here, the unit cell contained two molecules of **2** and six DMSO molecules (omitted from Figure 2B), all of which were hydrogen bonding directly to the N−H protons within the amidothiourea receptor. It was also clear, from these structures that the thiourea protons of the receptor moieties in both **2** and **6** occupy an anti conformation, but we had previously observed such geometry in the crystal structures of aminourea-based colorimetric sensors.[5g]

Spectroscopic Studies of Model Compounds 1 and 2 in Organic Solutions. As detailed above, the objective of the current study was to develop water-soluble anion receptors and test their anion recognition ability in competitive media, and compounds **1** and **2** were chosen as model compounds for this study, as both lack the water solubilizing groups introduced into **3**−**6**. Compound **2**, which contains a nitro substituent on each of the aryl part of the two amide thiourea moieties, should enable colorimetric changes, which should be visible to the naked eye upon anion recognition. Several research groups[16−21] have investigated the nature of such recognition processes in organic polar aprotic solvents such as DMSO, $CHCl_3$, or

dx.doi.org/10.1021/jo202332h | J. Org. Chem. 2012, 77, 3115−3126

CH_3CN for hydrogen-bonding receptors and various anions. We have shown that, in general, such binding interactions are dominated by hydrogen-bonding interactions. However, we have also shown that anion-induced deprotonations can occur, particularly for anions such as F^- and $H_2PO_4^-$ in such solvents.[5,6f,9,21] We have also demonstrated that it can be difficult to distinguish between these two processes using either UV−vis or fluorescence spectroscopic titrations, as the spectral changes are often similar and, in some cases, the same for both mechanisms. As such, various 1D and 2D ^{1}H NMR techniques have to be employed to elucidate the mechanism for such anion−host interactions. However, the concentration difference employed for these techniques differs greatly, which is an additional disadvantage. Hence, one of the objectives of developing **1** and **2** was also to attempt to distinguish between these two events as these two systems possess different electron withdrawing groups which are known to affect the acidity of the hydrogen donating receptors. Anion receptors possessing nitro groups can in particular give rise to deprotonation events. Therefore, compound **1**, possessing 4-trifluoromethylphenyl moiety, which at the same time as being highly electron withdrawing is also known to be less likely to induce deprotonation events for such amidothioureas, was also synthesized. Of these two systems, the discussion below will focus mostly on the results obtained from the titrations of **2** with various anions.

The absorption spectra of **2** in DMSO (1 μM) showed a broad absorption band centered at *ca.* 348 nm (ε = 21270 M^{-1} cm^{-1}), which we assigned to the internal charge transfer (ICT) character of the molecules, and a shoulder at shorter wavelength at ca. 290 nm, assigned to the pyridyl unit and higher energy bands associated with the nitrobenzene chromophore, Figure 3A. Upon excitation of **2** at the 348 nm band, the compound was found to be only slightly emissive, and hence, the following investigation only focuses on the anion-induced changes observed in the ground state of **2**. The compound was titrated with various anions (as their tetrabutylammonium, TBA, salts) such as AcO^- and $H_2PO_4^-$, $HP_2O_7^{3-}$, and F^-. For these titrations, upon increasing the anion concentration the recognition of the anions induced a bathochromic shift. In the case of phosphate, Figure 3A, a new band was formed at longer wavelength, centered at 420 nm, tailing into 560 nm, with the formation of an isosbestic point at 353 nm. These spectral changes demonstrated that the anion is bound within the receptor cleft, which is in conjugation to the *p*-nitrophenyl chromophore, and this binding enhances the strength of the ICT character with a concomitant shift in the absorption spectra to longer wavelengths. Importantly, these changes were also, even at such low concentration of the sensor, visible to the naked eye, changing from colorless to yellow. Similar changes were also observed in the absorption spectra of **1** using AcO^- (Figure 3B) and F^-, while only minor changes were observed in the absorption spectra using Cl^-, and no changes were observed using Br^-.

Analysis of the anion-induced changes in both **1** and **2** demonstrated that each of the amidothioureas was able to bind to a single anion, giving rise to an overall 1:2 binding stoichiometry, as shown as an inset in Figure 3A,B for the titration with $H_2PO_4^-$ and AcO^-, respectively. The relative changes in the absorption spectra of **2** at 425 nm are plotted against the added equivalents of these anions, Figure 4. These results indicate that F^- and AcO^- may, as did $H_2PO_4^-$, form hydrogen-bonded complexes with each amidothiourea arm of

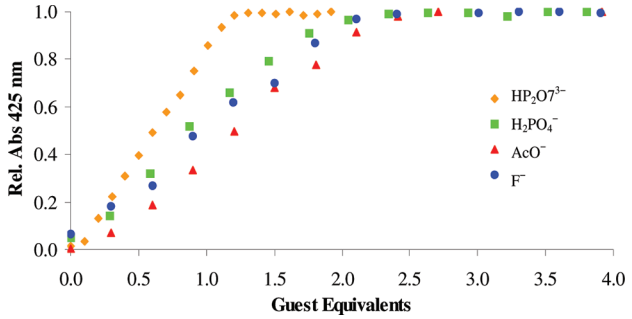

Figure 4. Relative changes in the absorption spectra of **2** (1×10^{-5} M) at 425 nm upon addition of various anions in DMSO.

the sensor, as a plateau was observed after the addition of ca. 2 equiv of each of these anions. Conversely, it was envisaged that ditopic anions such as $HP_2O_7^{3-}$ may bridge both arms of the sensor, thus giving rise to the observed 1:1 stoichiometry; hence, we next evaluated the ability of **1** to bind $HP_2O_7^{3-}$. Again, similar changes were observed in the absorption spectra of **1** as seen in Figure 3A upon binding to $HP_2O_7^{3-}$, and analysis of the spectral changes indeed demonstrated that the anion was bound in a 1:1 stoichiometry. Importantly the spectral changes were not reversed upon the addition of competitive hydrogen bonding solvents such as MeOH or H_2O, which strongly indicated that the anions could be detected in a mixture of organic−aqueous solution.

In the case of **1**, the titrations were carried out in DMSO/CH_3CN solution. Because of the nature of the receptor moiety, the absorption band occurred at higher energy in comparison to that seen for **2**, with a λ_{max} at 276 nm. However, upon titrations with various anions such as AcO^-, Figure 3B, the formation of a red-shifted transition was observed with a λ_{max} at 360 nm, and as in the case of **2**, the binding was found to be in a 1:2 (Host/Guest) stoichiometry (shown as inset in Figure 3B). However, analysis of the changes observed in the absorption spectra of both **1** and **2** by fitting the changes using the nonlinear regression analysis program SPECFIT, did not result in an accurate determination of binding constants for these changes, as these were all determined with large errors.[22] Because of this we investigated the binding phenomenon using NMR titrations.

^{1}H NMR Titration of 1 and 2 in DMSO-d_6. The above titrations showed that **1** and **2** could recognize various anions in 1:1 or 1:2 stoichiometries. While the changes in the absorption spectra are indicative of hydrogen bonding by these anions, it is not conclusive. Consequently, to shed light on the mechanism of action here, we carried out ^{1}H NMR titrations in DMSO-d_6 on **1** and **2** using the same anions as employed above. The changes in the ^{1}H NMR spectra of **2** upon titration with $H_2PO_4^-$ in DMSO-d_6 (see the Supporting Information) gave an indication of the general trend observed for these titrations. The first addition of $H_2PO_4^-$ (0.2 equivalents, not shown) resulted in the broadening of all the proton resonances. The intensity of the N−H amide proton, 11.30 ppm, decreased, and a new broad resonance was also observed slightly further downfield at ca. 11.8 ppm. Both thiourea protons also broadened before completely disappearing after the addition of 2 equiv of anion, along with a new signal at 11.8 ppm. At 1 equiv of $H_2PO_4^-$ a new signal also appeared at ca. 8.9 ppm, which gradually sharpened, along with the amide N−H signal, as the titration progressed. The resulting sharp resonances at 11.36 and 8.95 ppm were identified as N−H protons by

dx.doi.org/10.1021/jo202332h | J. Org. Chem. 2012, 77, 3115−3126

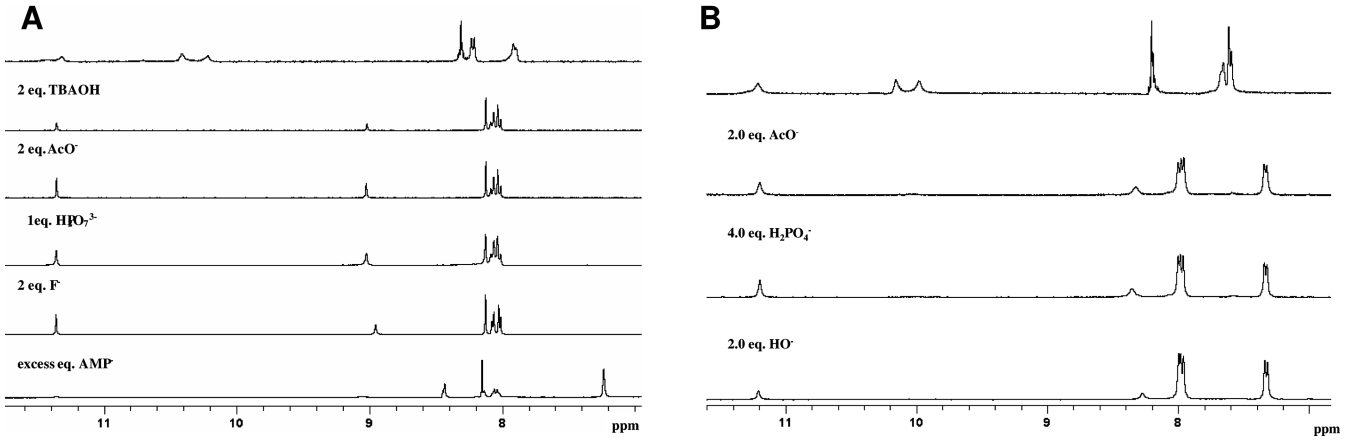

Figure 5. (A) Stack plot of **2** (top) and resulting spectra upon addition of various equivalents of anions in (600 MHz, DMSO-d_6). (B) Stack plot of changes in the ^{1}H NMR (400 MHz, DMSO-d_6) spectra of **1** upon addition of various anions.

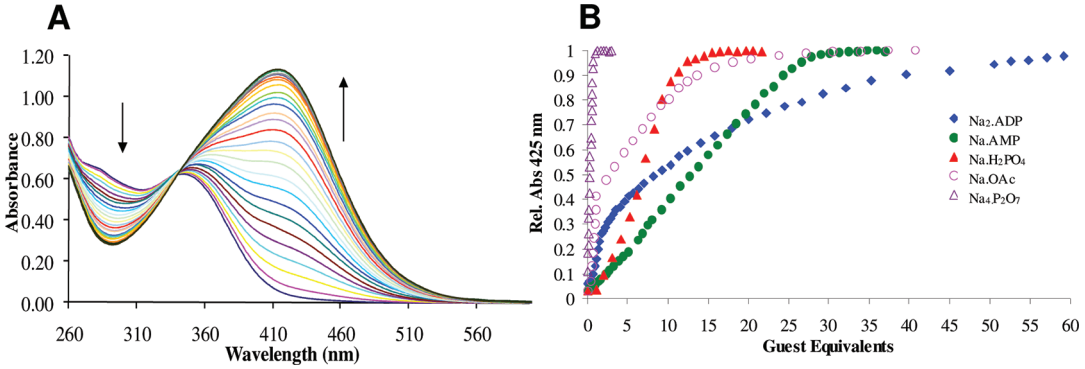

Figure 6. (A) Changes in the absorption spectra of **2** upon titration with AcO^- in 4:1 DMSO/H_2O solution. (B) Plot of the changes in the absorption of **2** upon addition of various phosphate-based anions in 4:1 DMSO/H_2O solution.

^{15}N–^{1}H COSY NMR, and both signals integrated for two protons each. In the case of the aromatic protons, the signals for the pyridine protons, as well as the *p*-nitrophenyl protons at ca. 8.22 ppm, were shifted upfield, while the *p*-nitrophenyl signal at 7.90 ppm was shifted downfield. Overall, these types of changes were indicative of deprotonation, as only four N–H protons were identified in the final spectrum, which might explain the difficulties encountered above when fitting the changes in the absorption spectra. Additionally, similar deprotonation patterns with pyrrole–amidothioureas have also been reported by Gale et al.[18] Figure 5A shows that titration of **2** with AcO^-, F^-, AMP^-, $HP_2O_7^{3-}$, and OH^- (all as TBA salts) also gave rise to a spectrum similar to that seen for $H_2PO_4^-$ above. Figure 5 also shows the number of equivalents of each anion that were required to produce the spectra above. Apart from $H_2PO_4^-$, these results are in close agreement with the number of equivalents required to reach a plateau in the absorption titrations in DMSO, shown previously in Figure 4, for **2**. In the case of **2**, we also carried out ^{1}H NMR titrations using AMP, which showed that a large excess of AMP was required to reach a plateau in comparison to the other anions. Hence, in DMSO solution, the recognition of these anions is most likely by hydrogen bonding between the receptor and the anions, which then at higher concentrations, gives rise to a full deprotonation event. In a similar manner the ^{1}H NMR of **1** was also recorded and the results in the presence of AcO^-, $H_2PO_4^-$, and F^-, Figure 5B, again indicted that the final species had the same common structure, and hence, supporting deprotonation as the likely mechanism in organic solvents. With this in mind we attempted to investigate the binding affinity of **1** and **2** in aqueous solution, which would suppress any such deprotonation mechanism.

Spectroscopic Studies of Model Compounds 1 and 2 in 4:1 DMSO/H_2O Solution. Because of the poor solubility of **1** and **2** in water or in alcoholic solutions, we were unable to carry out UV–vis anion titrations on these sensors in water or alcohol/aqueous solutions. Nevertheless, as **2** had been soluble in DMSO, we consequently carried out a preliminary investigation of **2** in an aqueous solution of DMSO where a 4:1 DMSO/H_2O mixture was found to give the best solubility for **2**, and this was also employed for **1**.

The changes observed in the absorption spectra of **2** were similar to those observed above in DMSO solution where the spectra were shifted to longer wavelengths upon interaction with anions such as AcO^-, Figure 6A, $H_2PO_4^-$ or F^-. Once more, no clear isosbestic point was observed for these changes. However a pseudo-isosbestic point was seen at ca. 340 nm in Figure 6A. However, on all occasions the number of equivalents required to reach a plateau (ca. 30 equiv) was higher than that required in DMSO (ca. 2 equiv). In the case of hydrogen bonding, this would be due to the competitive hydrogen-bonding nature of water. However, if deprotonation occurred, the higher concentration required would be due to the lower bascitiy of ions such as $H_2PO_4^-$, compared to hydroxide, which was also shown to give rise to a red shift in the absorption spectra of **2**. In a similar manner, the changes in the absorption

dx.doi.org/10.1021/jo202332h | J. Org. Chem. 2012, 77, 3115–3126

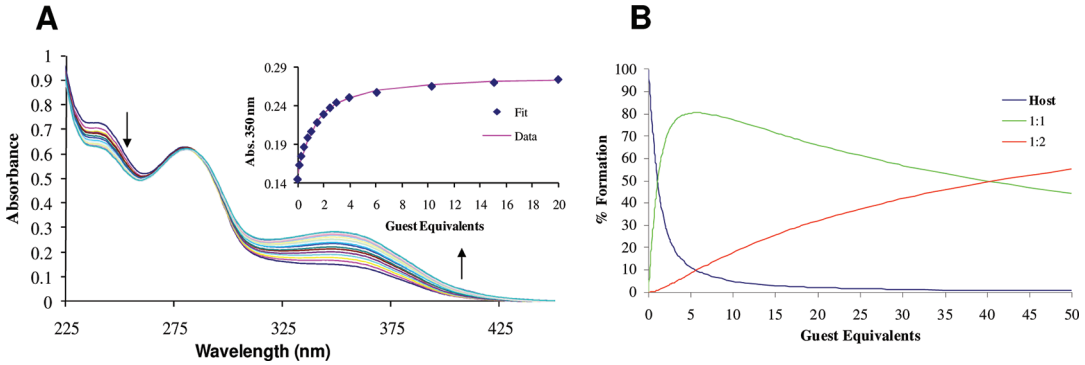

Figure 7. (A) Changes in the UV–vis absorption spectra of **3** in MeOH upon titration with acetate (TBAAc). (B) Species distribution diagram upon fitting the titration of **3** with AcO^- in MeOH to a 1:1 and 1:2 H/G binding model.

spectra of **1** was also affected upon binding to anions such as AcO^-, where a new transition was formed at 357 nm and a concomitant color change from colorless to yellow was observed. This clearly demonstrates that this receptor was also able to bind anions in this competitive media, at the same time as demonstrating that the nature of the electron-withdrawing group has significant effect on the changes in the absorption spectra.

Unlike that seen for the DMSO, analysis of these changes using the nonlinear regression analysis program SPECFIT did result in good fits to the experimental data of **2** (with the exception of F^-) from which binding constants and speciation distribution diagrams were determined. In the case of anions such as $H_2PO_4^-$, the changes in the absorption spectra were best fitted to both 1:1 and 1:2 Host/Guest stoichiometry, with binding constants of log $K_{1:1}$ = 4.24 (±0.06) and log $K_{1:2}$ = 4.07 (±0.04) determined for $H_2PO_4^-$. These values are close in magnitude, as expected for separated binding sites, one on each arm of the sensor. Similarly, high binding constants were determined for AcO^-, with log $K_{1:1}$ = 5.73 (±0.06) and log $K_{1:2}$ = 5.57 (±0.04).

Having demonstrated that **2** was able to bind these structurally simple anions, we next evaluated its ability further for the sensing of various biologically relevant phosphates, such as pyrophosphate, AMP, ADP, and ATP. Generally, with the exception of ATP, where no changes were observed in the absorption spectra, these titrations also gave rise to the formation of a new transition in the absorption spectra at long wavelengths with accompanied color changes, which were visible to the naked eye. Moreover, the spectral changes indicated a common mechanism of interaction of **2** with these anions. In the case of pyrophosphate, the spectral changes indicated a strong 1:1 binding interaction, which was also found to be the case for anions such as AMP and ADP. These results are summarized in Figure 6B as normalized changes in absorption vs anion equivalents. As before, the binding constants were determined for these interactions using nonlinear regression analysis. However, the best results were observed for $HP_2O_7^{3-}$ which gave a high binding constant for the 1:1 binding, with log $K_{1:1}$ = 6.53 (±0.3). The affinity of **1** for ADP was also high, but here the sensor was found to bind the $HP_2O_7^{3-}$ in both 1:1 and 1:2 stoichiometries, with log $K_{1:1}$ = 3.62 and log $K_{1:2}$ = 3.8, respectively.

While these results clearly indicate that sensors **1** and **2** were able to bind anions in highly competitive media, then the use of DMSO limits their use for practical purposes. Moreover, this high DMSO content can also favor a deprotonation event to occur, which is not desirable for sensing of biologically important anions. However, the above measurements using in particular **1** seem to indicate that this occurred to a lesser extent than using the nitro substituent **2**. Consequently, we made sensors **3**–**6** with the view of improving their use in more aqueous environments. However, judging from the above binding trends and affinities, we also anticipated that the binding of these modified versions would be lower in this competitive media.

Spectroscopic Studies of 3 and 4 in Alcoholic Solutions. Having been unable to fully study the sensing ability of **1** and **2** in competitive aqueous media, we embarked on the synthesis of a more "aqueous friendly" versions, namely **3**–**6**, the synthesis of which was described above. Because of the improved solubility of these compounds the anion-binding ability of **3** and **4** was first evaluated in MeOH and EtOH which are highly competitive medias for such hydrogen-bonding anion studies. Most of the discussion herein, however, focuses on the use of **3**, having the CF_3 substituent, as the results above suggested that the NO_2 substituent (i.e., compound **4**) would be more likely to give rise to deprotonation of the amidouthiourea protons due to a strong electron-withdrawing effect, as had been seen for **2** above. However, the use of the CF_3 group also has its drawbacks as the absorption spectra is blue-shifted in comparison to **2**, as we saw for **1** above. The absorption spectrum of **3** (ε = 26200 M^{-1} cm^{-1}, 275 nm) when recorded in MeOH is shown in Figure 7A and shows several transitions centered at 210, 240, 275, and 350 nm. While the transition centered at 350 nm was assigned to the ICT of the *p*-CF_3-phenyl chromophore, the band at ca. 275 nm was assigned to the n–π^* transitions of the pyridine moiety, and the band at 240 nm to the π–π^* transitions of both the pyridine and the *p*-CF_3-phenyl moieties. Figure 7A also shows the changes observed in the absorption spectra upon addition of acetate at 350 nm. Here, an increase in the ICT absorption band with a small concomitant decrease in the band centered at 240 nm was observed. In contrast, no changes were observed in the pyridine transition (275 nm) due to the interaction of AcO^- with the amidothiourea receptor moieties of **3**. Similar effects were also seen in EtOH solution when **3** was titrated with AcO^-. However, the changes were ca. 15% larger for the ICT band. The changes in the absorption spectrum of **3** in MeOH at 350 nm as a function of the equivalents added are shown as an insert in Figure 7A. As for **1** and **2**, these binding interactions were analyzed using the nonliner regression analysis program SPECFIT, which showed that the data was best fit (see solid line as inset in Figure 7A) to a 1:1 and then at higher

dx.doi.org/10.1021/jo202332h | J. Org. Chem. 2012, 77, 3115–3126

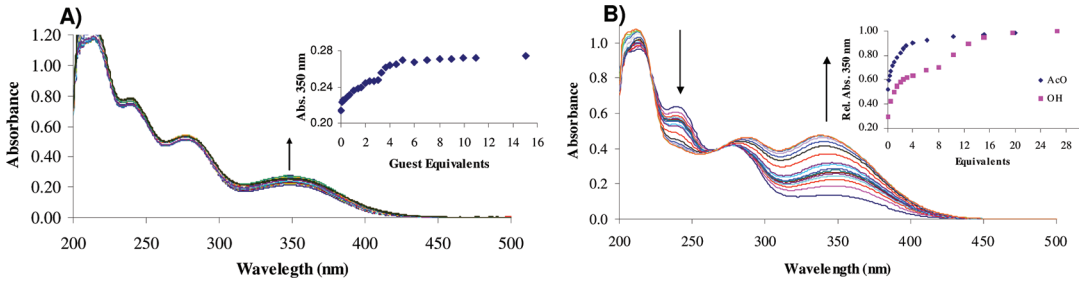

Figure 8. (A) Changes in the absorption spectrum of **3** (2.44×10^{-5} M) upon titration with F^- (0→16 equiv) in MeOH. (B) Changes in the absorption spectra of **3** upon titration with OH^-. Inset: Relative changes at 350 nm upon titration with AcO^- and OH^- as a function of equivalents.

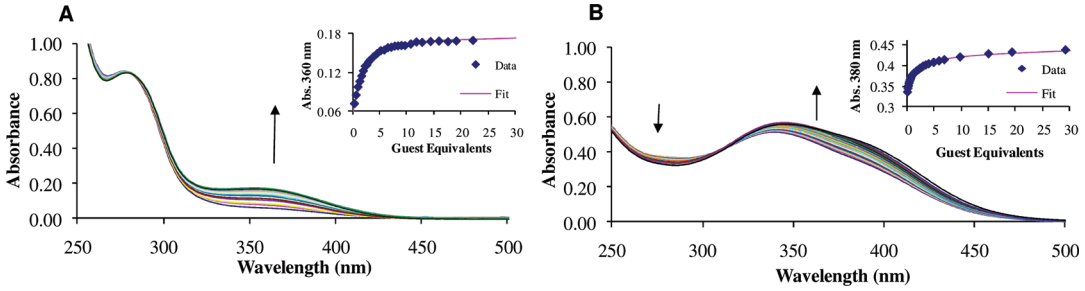

Figure 9. (A) Overall changes in the absorption spectra of **5** (1.55×10^{-5} M) in EtOH upon titration with $H_2PO_4^-$ (0 → 32 equiv). Inset: Changes at 360 nm with 1:1 fit (0 → 20 equiv) obtained from SPECFIT. (B) Changes in the absorption spectra of **6** (1.1×10^{-5} M) upon titration with AcO^- in MeOH. Inset: Changes at 380 nm with 1:2 H/G fit obtained from SPECFIT.

concentrations the 1:2 (Host/Guest) complex formation occurred, indicating that each of the amidothiourea moieties bound to a single anion for each of the pyridyl units. This fit resulted in binding constants of log $K_{1:1}$ = 4.9 (±0.1) and log $K_{1:2}$ = 3.0 (±0.4). This is the expected binding mode for such simple linear "Y"-shaped anions. In EtOH, the changes were also best fitted to a 1:2 (Host/Guest) stoichiometry, which gave a large 1:1 binding constant of log $K_{1:1}$ = 6.0 (±0.1). The 1:2 species, log $K_{1:2}$ = 2.8 (±0.3), was also found to be a minor species throughout the titration; not reaching more than 30% formation after the addition of 60 equiv of AcO^-, thereby demonstrating the effect the media has on recognition, Figure 7B.

Because of the high binding affinity observed for AcO^-, sensor **3** was also titrated with the TBA salts of F^- and $H_2PO_4^-$ in MeOH. Changes similar to those observed for AcO^- occurred in the presence of F^-; however, these changes were smaller in magnitude (ca. 50%) and did not reach a plateau until after the addition of ca. 5 equiv of the anion, Figure 8A. The reason for this is most likely the high solvation energy associated with F^- in this media, which will make it very difficult to overcome.

Surprisingly, the titration of **3** with $H_2PO_4^-$ resulted in a minor increase in the ICT transition, which after the addition of 5 equiv began to decrease in absorption with a concomitant minor bathochromic shift. Unfortunately, the changes in the presence of F^- and $H_2PO_4^-$ could not be accurately fitted using nonlinear regression analysis. It is likely that this could possibly be due to some contribution from a deprotonation event which can give rise to "false-positive" responses, as we have discussed above for **1**[11,19] and **2**. The occurrence of a possible deprotonation of the sensor **3** by these anions was thus investigated by using TBAOH in MeOH. The changes in the absorption spectrum of **3**, Figure 8B, were considerably larger than those seen upon titration of **3** with AcO^-, with significant changes occurring at both the 240 and 350 nm transitions, with the formation of an isosbestic point at ca. 266 nm, after the addition of ca. 6 equiv of OH^-.

Whereas large changes were seen for **2**, possessing the nitro substituent, only minor changes were seen in the absorption spectra of **4** (ε = 36950 M^{-1} cm^{-1} at 339 nm) when similar anion titrations were carried out in this media (see Figures S10 and S11, Supporting Information). This clearly suggests that the chain on the 4-position of the pyridyl unit does influence the sensing ability of these structures, as well as the nature of the substituent and the media; and while this could have been anticipated, the difference observed here is significantly greater than we had foreseen. Nevertheless, we were able to determine the binding constants for the binding of **4** to these anions. The changes in the presence of AcO^- and F^- were fitted best to 1:1 and to 1:2 stoichiometry which gave binding constants of log $K_{1:1}$ = 5.60 (±0.07) and log $K_{1:2}$ = 3.6 (±0.1) for AcO^- and log $K_{1:1}$ = 4.8 (±0.1) and log $K_{1:2}$ = 3.6 (±0.2) for F^-. In comparison to the fitting of **3** with AcO^-, the species distribution diagrams for **4** upon titration with both AcO^- and F^- showed a larger contribution from the 1:2 species (see Figures S12 and S13, Supporting Information). This could be due to the presence of the nitro groups, which, as discussed above, makes the N–H protons more acidic and, hence, better hydrogen bond donors, or conversely, easier to deprotonate.

Spectroscopic Studies of 5 and 6 in Alcoholic Solutions. In a similar manner, **5** and **6** were also titrated using various anions in MeOH and in EtOH solutions.[26] Similar changes were observed for **5** as were seen for **3** for AcO^- and F^-. However, the analyses of changes induced by $H_2PO_4^-$, Figure 9, showed that only the 1:1 binding (log $K_{1:1}$= 4.55 (±0.03)) gave rise to the main changes in the absorption spectra, with minor changes occurring up to the addition of two equivalents (Figure S14, Supporting Information), as seen in the Figure 9 inset. However, the largest changes occurred up to the addition of 1 equiv of $H_2PO_4^-$ and reached a plateau at ca. 2 equiv. Sensor **5** was also titrated with AcO^- in MeOH, which

dx.doi.org/10.1021/jo202332h | J. Org. Chem. 2012, 77, 3115–3126

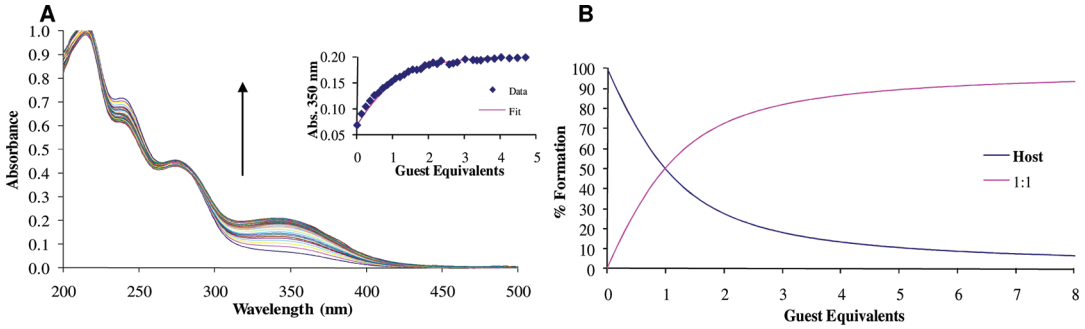

Figure 10. (A) Overall changes in the absorption spectra of **3** (1.65×10^{-5} M) upon titration with $H_2PO_4^-$ (0 → 8.5 equiv) in 1:1 EtOH−H_2O. Inset: Changes at 350 nm with a 1:1 fit obtained from SPECFIT. (B) Species distribution diagram obtained from the fitting of the titration of **3** with $H_2PO_4^-$ in 1:1 EtOH−H_2O to a 1:1 binding stoichiometry.

gave rise to similar changes to those seen in the absorption spectra of **1**; these changes were best fitted to both 1:1 and to 1:2 stoichiometry using SPECFIT, which gave binding constants of log $K_{1:1}$ = 5.00 (±0.04) and log $K_{1:2}$= 3.1 (±0.1). The log $K_{1:1}$ value was similar to that seen for **1** upon titration with AcO^- in MeOH (log $K_{1:1}$= 4.86 (±0.04)). Sensor **5** was also titrated with TBAOH and HSO_4^- in MeOH, which resulted in a large increase and decrease in the ICT transition of the absorption spectra. This is most likely due to deprotonation and protonation of the receptor moieties by these anions, respectively.[23]

Spectroscopic changes similar to to that seen for **1** were observed upon titration of **6** with AcO^-, but here the AcO^- and F^- titrations were also best fitted to a 1:1 stoichiometry model, which resulted in binding constants of log $K_{1:1}$= 6.3 (±0.3) and log $K_{1:1}$= 5.59 (±0.2), respectively. This log $K_{1:1}$ value was close in magnitude to that determined for **1** with AcO^- in EtOH. Sensor **6** was also titrated with AMP, ADP, and ATP in EtOH. In the case of AMP, slightly larger changes were seen in the ICT transition of the absorption spectrum compared to those seen for AcO^-, $H_2PO_4^-$, and F^-. However, these changes did not reach a plateau until after the addition of ca. 80 equiv of AMP, at which point the absorption of the AMP began to overlap with the changes in the ICT transition of **6**. The changes in the presence of AMP were fitted using SPECFIT, from which the best fit was for a 1:1 stoichiometry, giving log $K_{1:1}$ = 3.67 (±0.03) for the binding of AMP. In comparison to the changes in the presence of AMP, only minor changes occurred in the presence of ADP, and titration with ATP did not result in a decrease in the absorption of the ICT transition as had been seen for the previous sensors. In the case of hydrogen bonding, the absence of any significant spectral changes suggested that ADP may be too large to interact in a favorable manner with the sensor. This may indicate that a cavity or "binding pocket" was formed by the sensor in solution, such as that seen in the crystal structure of **6**. The increase in the absorption of the ICT transition of **6** upon titration with anions in EtOH indicated a common mechanism of anion interaction to that seen for sensors **1** and **2**. The spectral changes in the presence of $HP_2O_7^{3-}$ were similar to those observed upon titration of **1** with $HP_2O_7^{3-}$ and TBAOH in 1:1 EtOH−H_2O solution. These changes were previously assigned to deprotonation of the receptor moieties of **1**, as a large increase in the pH of the solution was measured. Therefore, it is quite likely that the overall changes in the absorption spectrum of **6** upon titration with $HP_2O_7^{3-}$ were also due to deprotonation of the N−H protons. Although these changes could not be fitted using SPECFIT, the evolving factor analysis (EFA) estimated the presence of three colored species in solution, including sensor **6**. The other two species most likely resulted from the deprotonation of the receptor moieties of **6**. In support of the latter explanation, the titration of **6** with TBAOH resulted in large changes in the absorption spectrum, the magnitude of which were similar to those seen in the presence of $HP_2O_7^{3-}$.[24,25]

Spectroscopic Studies of 3 and 4 in 1:1 Alcoholic/H_2O Solutions. Having investigated the changes of **3**−**6** in alcoholic solutions, we next investigated these in a more competitive 1:1 EtOH:/H_2O mixture. The absorption spectrum of **3** (ε = 25950 M^{-1} cm^{-1}, 280 nm) in 1:1 EtOH−H_2O solution was similar to that observed in EtOH. As before, the addition of anions such as AcO^-, $H_2PO_4^-$, and F^- to this solution resulted in a modulation of the ICT transition of the sensor to **3** (see Figures S15 and S16, Supporting Information) in this competitive media, resulted in a modulation of the ICT transition of the sensor, which was found to be most pronounced for the titration with $H_2PO_4^-$, Figure 10A. The insert in Figure 10A shows that 2 equiv of the anion were necessary to reach a plateau; however, these changes were best fitted to a 1:1 binding stoichiometry using SPECFIT, and in this case, no 1:2 species was observed, Figure 10B. This clearly demonstrated the sensing ability of these structures, even in highly competitive media. Unlike that seen above, these changes were best fitted to a 1:1 binding stoichiometry, with a log $K_{1:1}$ = 5.12 (±0.09), indicating a strong binding affinity for $H_2PO_4^-$. Similarly **4** gave log $K_{1:1}$ = 5.46 (±0.07) for $H_2PO_4^-$. If this species is due to the formation of a hydrogen-bonded complex between the sensor and this anion, it is possible that the 1:1 binding stoichiometry was favored due to the formation of a hydrophobic cleft within the structure of **3**, as previously postulated by Jiang et al. for monoamidothiourea sensors.[8,16] For AcO^-, 2 equiv of the anion were required to reach a plateau for **3** and **4**; nevertheless, these changes were best fitted to 1:1 binding with log $K_{1:1}$ = 5.58 (±0.05) for **4**. Despite the more competitive solvent system employed here, the binding constant determined for AcO^- was similar to that determined in MeOH for **3**. It is, however, important to point out that the pH of the 1:1 solution changed by ca. 0.2−0.3 pH units upon addition of 10 equiv of these anions, indicating that these anions were recognized dominantly by **3** and **4** through hydrogen-bonding interactions. In the case of F^-, ca. 15 equiv was required to reach a plateau in **3**, while the titration of **4** with F^- required ca. 4 equiv. As above, the pH of the solution did not change during the titration (see Table S1, Supporting

dx.doi.org/10.1021/jo202332h | J. Org. Chem. 2012, 77, 3115−3126

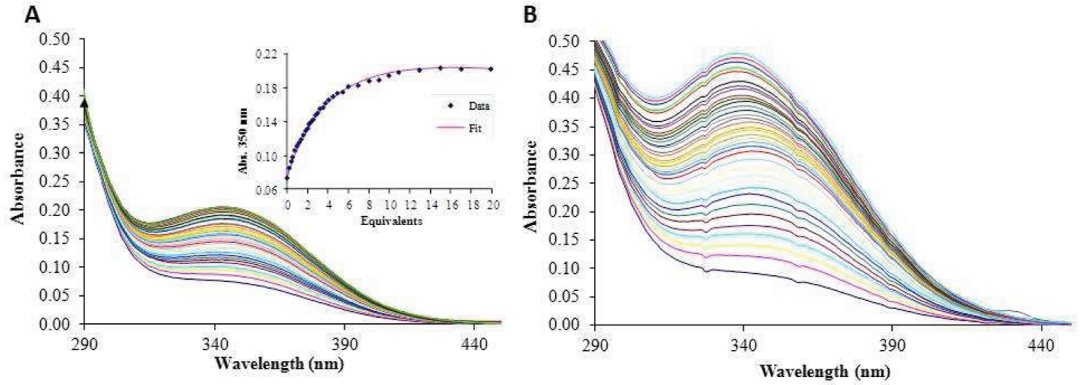

Figure 11. (A) Changes in the long-wavelength ICT band in the UV–vis absorption spectra of **3** in 1:1 EtOH/H_2O upon titration with AMP. Inset: Binding isotherm and fitted 1:1 data. (B) Changes in the IC- based absorption band of **4** in the presence of pyrophosphate in the same solvent system.

Information). From these results, it is possible that the strong interaction with $H_2PO_4^-$ may be due to the fact that the tetrahedral anion could more easily bridge both arms of the sensor, in comparison to the planar AcO^- anion or the small spherical F^- anion (also more hydrated in this solvent system). In contrast to these changes, no changes were seen in the absorption spectrum of **3** upon titration with Cl^-, Br^-, and I^-.

Because of the dominant 1:1 binding of AcO^- and $H_2PO_4^-$ in aqueous solution, we also evaluated the sensitivities of these sensors toward biologically relevant phosphates such as pyrophophate ($HP_2O_7^{3-}$), AMP, ADP, and ATP for both **3** and **4**. The changes seen for the titration of **3** with AMP and $HP_2O_7^{3-}$ are shown in parts A and B of Figure 11, respectively, and clearly show that the long wavelength absorption band underwent significant changes upon binding of both of these anions, which on both occasions was significantly greater in magnitude than seen for the more structurally simpler anions. Analysis of these changes using nonlinear regression analysis clearly showed the initial formation of a 1:1 complex, but after the addition of 15 equiv, both 1:1 and 1:2 complexes were formed in equal amount; and in fact, the overall spectral changes were best fitted to a 1:2 stoichiometry with log $K_{1:1}$ = 5.58 (±0.07) and log $K_{1:2}$ 3.64 (±0.09) for these changes. However, the pH of this solution, after the addition of just three equiv. of $HP_2O_7^{3-}$, changed by ca. 0.7 pH units, which indicates that a deprotonation of the sensor by the anion may be contributing to these spectral changes as well.

Similarly, significant spectral changes were seen for the titration of **3** using AMP, ADP, and ATP. For AMP (Figure 11A) and ADP the ICT band of **3** increased in absorption in a similar manner to that seen above in Figure 7, and the changes were similar in magnitude; AMP giving slightly greater changes in the absorption at 350 nm. The changes were best fitted to a 1:1 stoichiometry which gave log $K_{1:1}$ = 4.02 (±0.12) and 3.63 (±0.12) for these anions, respectively, showing that AMP was bound with slight preference over ADP. Importantly, in comparison to that seen for pyrophosphate, only minor pH changes were observed (ca. 0.2 pH units) for these titrations. This suggests that the changes observed are more likely due to the formation of hydrogen-bonded complexes between the sensor and these anions, rather than the occurrence of deprotonation. In contrast, the titration of ATP gave rise to a decrease in the λ_{max}, and the pH of the solution had changed to pH 4.5 (±0.1) at the end point. Hence, from these results it is possible to state that **3** can selectively recognize AMP and ADP over ATP, where the selectivity is in favor of AMP over ADP. In a similar manner, compound **4** was titrated with various anions, and in general, these changes were less than seen for **3**, confirming the same trend as seen for the structurally simple anions above.

The absorption spectra of **5** and **6** in 1:1 EtOH–H_2O (and 1:1 MeOH–H_2O) solutions, respectively, were similar to their corresponding spectra in alcohol. Titration of **5** with $H_2PO_4^-$ resulted in a different pattern of change to that observed for the previous sensors and a decrease in the absorptions centered at 210, 240, and 280 nm was observed. However, upon the addition of 0.8 equivalents of $H_2PO_4^-$, a white precipitate was visible in solution. This indicated that the initial decreases in the absorption spectrum were also as a result of precipitation of these sensors from solution. As discussed above, the solubility of sensors **5** and **6** in alcohol were lower than that of **3** and **4**, and while it was anticipated that an "anion binding pocket" may be formed in solution by the tetraamidothiourea sensors, such interactions may also result in an increase of stacking interactions in solution and, hence, lower the solubility of the compounds. As the studies carried out on the tetraamidothiourea sensors in alcohol showed more or less similar spectral responses to their corresponding bis analogues, it was decided not to investigate the anion binding capabilities of **5** and **6** in more competitive media any further.[27]

■ CONCLUSION

In this paper, we present the synthesis and discuss the spectroscopic results from six new anion receptors, **1**–**6**, based on cleftlike structures where the anion recognition occurs through the synergetic action of two or more amiothiourea moieties with various anions. We also demonstrated that caution must to be paid to the elucidation of the mechanism for such anion sensing; as hydrogen bonding and deprotonation can both contribute to the overall anion sensing mechanism. We show that the structures possessing glycol chains, **3**–**6**, enable us to evaluate their use for anion recognition in alcohol or competitive aqueous/alcohol solutions, while compounds **1** and **2**, which lack these chains, could only be studied in organic solutions such as DMSO. The structural modification of **3**–**6** proved particularly successful for both **3** and **4**, which were titrated with various anions in both alcohol and alcohol–water mixtures, while the larger tetra amido-thiourea systems **5** and **6** were only partially soluble in alcohol–water mixtures and, hence, were only titrated in alcohol solutions. The anion-

dx.doi.org/10.1021/jo202332h | J. Org. Chem. 2012, 77, 3115–3126

binding capabilities of **3** and **4** were initially assessed in either or both MeOH and EtOH solution by titrating these compounds with AcO^-, $H_2PO_4^-$, and F^-, respectively. The results from these titrations showed that both sensors interacted most strongly with AcO^-, with large 1:1 binding constants determined from nonliner regression analysis, using SPECFIT. Additionally, the control titrations carried out with base suggested that these changes could be due to the formation of hydrogen bonded complexes, as the changes in the presence of base were far larger in magnitude. In comparison to the changes observed in the absorption spectra of both **3** and **4** with AcO^- and F^-, the spectral changes in the presence of $H_2PO_4^-$ were different, whereby an increase in the absorption followed by a decrease and bathochromic shift occurred. This indicated that the nature of the hydrogen-bonded complex formed with the tetrahedral anion was quite different to that of AcO^- and F^-. Working towards achieving anion binding in highly competitive media, compounds **3** and **4** were then titrated with the aforementioned anions in mixtures of alcohol and water solutions. These titrations resulted, on all occasions, in an increase in the ICT transition of both **3** and **4** in the presence of AcO^-, $H_2PO_4^-$ and F^-. In the case of **3**, strong recognition of $H_2PO_4^-$ was shown to occur in 1:1 EtOH-H_2O solution, as a high binding constant was determined by fitting the overall changes in the absorption spectra. In order to better understand the anion interactions of **3** and **4** in 1:1 EtOH–H_2O and 1:1 MeOH–H_2O solutions, spectroscopic pH titrations were carried out. The results from these titrations gave a further understanding of these sensors in solution and the effect that pH had on the changes in the absorption spectra. These experiments showed that the pK_{a1} values of these sensors were quite low (ca. 6 for both **3** and **4**). These values initially caused concern that the receptor moieties of **3** and **4** may be deprotonated by anions too easily. However, despite the low pK_{a1} determined, only minor changes in the pH (ca. 0.3) were measured upon the addition of anions such as AcO^-, $H_2PO_4^-$ and F^- to mixed alcohol–water solutions of **3** and **4**. These results supported the formation of hydrogen-bonded complexes in these solvent systems. Additionally, the changes observed in these titrations were fitted to 1:1 stoichiometries, while those in 100% alcohol were fitted to both 1:1 and to 1:2 stoichiometries. This may indicate that there was a minor contribution from deprotonation in the less competitive alcohol solutions. Compounds **3** and **4** were also titrated with "larger" biologically important phosphate-based anions, such as AMP, ADP, ATP, and $HP_2O_7^{3-}$. The largest changes were seen for $HP_2O_7^{3-}$, where the overall changes in the presence of $HP_2O_7^{3-}$ were assigned to some degree of deprotonation for both **3** and **4** (with a change in the pH of the solution of 0.7). In contrast to these changes, smaller spectral changes were seen in the ICT transitions of **3** and **4** upon addition of AMP and ADP. These changes gave rise to minor changes in the pH of ca. 0.2 pH units and in the case of **3** were best fitted to a 1:1 stoichiometry. In contrast to these results, the addition of ATP resulted in a decrease in the ICT transition of the absorption spectra of both **3** and **4** as well as a substantial decrease in the pH. Titrations of the tetraamidothiourea sensors, **5** and **6** with various anions also gave rise to an increase in the ICT band in the absorption spectra, in a similar manner to that seen for **3** and **4** in EtOH and MeOH, respectively. However, the changes in the presence of AcO^-, $H_2PO_4^-$, and F^- were smaller in magnitude when compared to those seen for **3**. It was hoped that these sensors could detect the presence of anions more strongly than **3** and **4** due to the cooperative binding of anions by all four receptor moieties within a "binding pocket". The main species observed upon fitting the titrations of **5** with AcO^-, $H_2PO_4^-$, F^-, and AMP was a 1:1 stoichiometric species, as had been seen for the bis-systems earlier. In the case of AcO^-, the binding constant with **5** was comparable to that observed for **3** in EtOH. Hence, these binding constants did not indicate a cooperative effect for the recognition of AcO^-. Unfortunately, the solubility of these compounds in 1:1 alcohol–water solutions was lower than anticipated, making the preparation of such solutions difficult. Because of solubility issues and the fact that the general trends of the spectroscopic changes were similar to those observed for the **3** and **4**, the anion-sensing capabilities of these sensors were not investigated in mixed alcohol–water solutions. We are currently developing other analogues of **3** and **4** with the view of further improving their water solubility and evaluating their ability to transport phosphate-based anions between different solvent systems and through bilayers.

EXPERIMENTAL SECTION

Diethyl 4-(2-(2-Methoxyethoxy)ethoxy)pyridine-2,6-dicarboxylate (10). Compound **9** (0.300 g, 1.26 mmol) and anhydrous K_2CO_3 (0.174 g, 1.26 mmol) were stirred in anhydrous DMF (9 mL) at 25 °C for 0.5 h. 1-Iodo-2-(2- methoxyethoxy)ethane (0.264 g, 1.14 mmol) was added and the solution was heated at 50 ° C for 50 h. The solvent was then removed under reduced pressure, and DCM (20 mL) was added to the residue. The organic layer was washed with 1% acetic acid (5 mL) and H_2O (5 mL). The organic layer was dried over $MgSO_4$, and the solvent was removed under reduced pressure to give **10** as a white solid (0.263 g, 67%): mp 200–203 °C dec; HRMS (ES^+) calcd for $[M + H]^+$ $C_{16}H_{24}NO_7$ 342.1548, found 342.1553; δ_H (400 MHz, $CDCl_3$) 7.82 (2H, s, CH_{py}), 4.48 (4H, q, J = 7.0 Hz, CH_{2ester}), 4.33 (2H, t, J = 4.5 Hz, CH_2), 3.93 (2H, t, J = 4.5 Hz, CH_2), 3.73–3.72 (2H, m, CH_2), 3.59 (2H, t, J = 4.5 Hz, CH_2) 3.40 (3 H, s, OCH_3), 1.47 (6 H, t, J = 7.0 Hz, CH_3); δ_C (100 MHz, $CDCl_3$) 166.7 (q), 162.5 (C═O), 150.1 (q), 114.4 (CH), 71.9 (CH_2), 70.9 (CH_2), 69.1 (CH_2), 68.2 (CH_2), 62.4 (OCH_2), 59.1 (OCH_3), 14.2 (CH_3).

4-(2-(2-Methoxyethoxy)ethoxy)pyridine-2,6-dicarbohydrazide (11). Compound **10** (0.263 g, 0.770 mmol) and hydrazine monohydrate (0.197 g, 6.16 mmol, 0.19 mL) were stirred at reflux in EtOH (40 mL) overnight. The resulting precipitate was isolated by suction filtration and washed with EtOH (2 × 20 mL) to give **11** as a white solid (0.094 g, 51%): mp 137–140 °C; HRMS (ES^+) calcd for $C_{12}H_{19}N_5O_5Na$ $[M + Na]^+$ 336.1284, found 336.1278; δ_H (400 MHz, DMSO-d_6) 10.60 (2H, br s, NH_{amide}), 7.60 (2H, s, CH_{py}), 4.62 (4H, br s, NH_2), 4.32 (2H, t, J = 4.1 Hz, CH_2), 3.77 (2H, t, J = 4.5 Hz CH_2), 3.60–3.58 (2H, m, CH_2), 3.46–3.43 (2H, m, CH_2), 3.23 (3H, s, OCH_3); δ_c (400 MHz, DMSO-d_6) 166.9 (q), 161.6 (C═O), 150.5 (q), 109.6 (CH), 71.2 (CH_2), 69.7 (CH_2), 68.4 (CH_2), 68.0 (CH_2), 58.0 (CH_3); IR ν_{max} (cm^{-1}) 3489, 3321, 3100, 2904, 1651, 1596, 1536, 1511, 1442, 1365, 1348, 1285, 1257, 1165, 1135, 1112, 1096, 1048, 996, 933, 880, 826, 746, 688.

4,4′-((Ethoxyethoxy)ethyl)bis[diethyl ester-2,6-pyridine] (12). Compound **9** (0.200 g, 0.836 mmol) and anhydrous K_2CO_3 (0.115 g, 0.836 mmol) were stirred in anhydrous DMF (60 mL) at 25 °C for 0.5 h. Di(iodoethoxy)ethane (0.154 g, 0.418 mmol) was added, and the solution was heated at 50 ° C for 50 h. The solvent was then removed under reduced pressure, and DCM (50 mL) was added to the residue. The organic layer was washed with 1% acetic acid (25 mL) followed by H_2O (25 mL). The organic layer was dried with $MgSO_4$, and the solvent was removed under reduced pressure to give yellow oil. The crude product was recrystallized from EtOH giving **12** as a white solid (0.147 g, 41%): mp 75–76 °C; HRMS (ES^+) calcd for $C_{28}H_{36}N_2O_{12}Na$ $[M + Na]^+$ 615.2166, found 615.2169; δ_H (400 MHz, $CDCl_3$) 7.78 (4H, s, CH_{py}), 4.42 (8H, q, J = 7.0 Hz, CH_2OCH_3), 4.28 (4H, t, J = 4.5 Hz, CH_2), 3.88 (4H, t, J = 4.4 Hz, CH_2), 3.72 (4H, s, CH_2), 1.41 (12 H, t, J = 7.2 Hz, CH_3); δ_C (100 MHz, $CDCl_3$) 166.7

dx.doi.org/10.1021/jo202332h | J. Org. Chem. 2012, 77, 3115–3126

(q), 164.6 (C=O), 150.1 (q), 114.4 (CH), 70.9 (CH_2), 69.2 (CH_2), 68.2 (CH_2), 62.4 (CH_2), 14.1 (CH_3); IR ν_{max} (cm^{-1}) 3076, 2983, 2933, 2905, 1742, 1706, 1594, 1567, 1478, 1435, 1369, 1371, 1342, 1328, 1244, 1230, 1158, 1134, 1102, 1067, 1023, 994, 938, 887, 866, 817, 786, 732, 701.

4,4′-(Ethoxyethoxy)ethyl)bis[dihydrazide-2,6-pyridine] (13). Compound **12** (0.500 g, 0.84 mmol) and hydrazine monohydrate (0.540 g, 16.86 mmol) were refluxed in anhydrous EtOH (300 mL) for 2 days. The white precipitate was collected by suction filtration giving **13** as a white solid (0.367 g, 81%): mp 200−203 °C dec;δ_H (400 MHz, DMSO-d_6) 10.59 (4H, br s, NH_{amide}), 7.59 (4H, s, CH_{py}), 4.61 (8H, br s, NH_2), 4.32 (4H, br s, CH_2), 3.78 (4H, br s, CH_2), 3.62 (4H, s, CH_2); δ_C (100 MHz, DMSO-d_6) 167.4 (q), 162.1 (C=O), 150.9 (q), 110.1 (CH), 70.4 (CH_2), 69.0 (CH_2), 68.5 (CH_2); δ_N (60 MHz, DMSO-d_6) 129.6, 135.6; IR ν_{max} (cm^{-1}) 3304, 3078, 2929, 1654, 1587, 1520, 1434, 1374, 1352, 1322, 1244, 1170, 1124, 1109, 1062, 1050, 992, 946, 912, 889, 823, 747.

General Procedure for the Synthesis of Amidothioureas. A solution of the isocyanate (2 equivalents) in CH_3CN was added to a solution of the dihydrazide (1 equiv) in CH_3CN. The reaction mixture was refluxed under argon for 16 h. The precipitate was then isolated by suction filtration and washed several times with warm CH_3CN. The resulting solid was dried under vacuum.

2,6-Bis[4-trifluoromethylphenyl(thioureidocarbomoyl)]-pyridine (1). Compound **1** was synthesized according to above procedure using **8** (0.150 g, 0.769 mmol) and 4-trifluoromethylphenyl isothiocyanate (0.312 g, 1.53 mol) in CH_3CN (50 mL), yielding **1** as a white solid (0.360 g, 77%): mp >300 °C; HRMS (ES^-) calcd for $C_{23}H_{16}N_7O_2S_2F_6$ $[M - H]^-$ 600.0711, found 600.0686; δ_H (400 MHz, DMSO-d_6) 11.30 (2H, br s, NH_{amide}), 10.24 (2H, br s, NH_{urea}), 10.06 (2H, br s, NH_{urea}), 8.21−8.17 (3H, m, H_{py}), 7.67−7.74 (8H, m, Ar-*H*); δ_C (100 MHz, DMSO-d_6), 181.1 (C=S), 162.8 (C=O), 147.7 (q), 142.9 (q), 139.6 (CH), 126.1 (CH), 125.5 (CH), 125.4 (CH), 124.2 (CF_3,J_{13C9F} = 273.1 Hz), 122.2 (q); δ_N (60 MHz, DMSO-d_6) 129.3, 124.2, 126.6; δ_F (162 MHz DMSO-d_6) −61.0; IR ν_{max} (cm^{-1}) 3368, 3134, 2962, 1705, 1617, 1601, 1541, 1463, 1415, 1328, 1278, 1217, 1156, 1105, 1065, 1016, 1000, 931, 886, 838, 786, 745, 725, 685. Anal. Calcd for $C_{23}H_{17}F_6N_7O_2S_2$: C, 45.92; H, 2.85; N, 16.30. Found: C, 45.79; H, 2.88; N, 16.10.

1,6-Bis[4-nitrophenyl(thioureidocarbomoyl)]pyridine (2). Compound **2** was synthesized according to the above procedure using **8** (0.281 g, 1.03 mmol, 1 equiv) and 4-nitrophenyl isothiocyanate (0.518 g, 2.88 mmol, 2 equiv) and then refluxed for 16 h. The precipitate was isolated by suction filtration and washed with acetonitrile to give a pale yellow solid, 0.784 g, 98%: mp 203.8−205 °C; δ_H (600 MHz, DMSO-d_6) 11.30 (2H, br s, $NHNH_{urea}$), 10. 37 (2H, br s, NH_{urea}), 10.20 (2H, br s, NH_{urea}), 8.31 (2H, br s, *CH*py), 8.30 (1H, br s, *CH*py), 8.22 (4H, br s, *CH*CNO_2), 7.92 (4H, br s, Hz, *CH*CNH); δ_C (100 MHz DMSO-d_6) 181.1 (C=S), 162.8 (C=O), 147.8 (C3), 145.7 (CNH), 143.6 (CNO_2), 139.8 (C5), 125.6 (C4), 125.2 (CHCNH), 123.9 ($CHCNO_2$); υ_N (600 MHz DMSO-d_6) 129.6, 127.7, 126.2; IR ν_{max} (cm^{-1}) 3128, 2962, 1704, 1597, 1549, 1506, 1469, 1345, 1278, 1219, 1157, 1002, 887, 851, 745, 698; HRMS (ES^+) calcd for $C_{21}H_{18}N_9O_6S_2$ 556.0821, found 556.0822 (M + H).

4-(2-(2-Methoxyethoxy)ethoxy)-2,6-bis-[4-trifluoromethylphenyl(thioureidocarbomoyl)]pyridine (3). Compound **3** was synthesized according to the above procedure using **11** (0.113 g, 0.360 mmol) and 4-trifluoromethylphenyl isothiocyanate (0.144 g, 0.720 mmol) in CH_3CN (20 mL). A white solid was obtained (0.172 g, 66.4%): mp 200−212 °C dec; HRMS ($MALDI^+$) calcd for $C_{28}H_{28}N_7O_5F_6S_2$ $[M + H]^+$ 720.1498, found 720.1533; δ_H (400 MHz, DMSO-d_6) 11.25 (2H, br s, NH_{amide}), 10.19 (2H, br s, NH_{urea}), 10.04 (2H, br s, NH_{urea}), 7.67−7.74 (10H, br m, Ar-H), 4.39 (2H, br s, CH_2), 3.80 (2H, br s, CH_2), 3.60 (2H, m, CH_2), 3.46 (2H, m, CH_2), 3.24 (3H, s, OCH_3); δ_C (100 MHz, DMSO-d_6) 181.5 (C=S), 167.4 (q), 162.9 (C=O), 150.2 (q), 143.2 (q), 126.0 (CH), 125.5 (CH), 125.3 (CH), 124.6 (CF_3, J_{13C9F} = 273.1 Hz), 122.5 (q), 111.3 (CH), 71.5 (CH_2), 70.5 (CH_2), 68.8 (CH_2), 58.3 (OCH_3); δ_F (376 MHz, DMSO-d_6) −61.0 (CF_3); IR ν_{max} (cm^{-1}) 3139, 2947, 1711, 1602, 1583, 1479, 1321, 1277, 1108, 1066, 892, 839. Anal. Calcd for $C_{28}H_{27}F_6N_7O_5S_2$: C, 46.73 H, 3.78 N, 13.57. Found: C, 46.43; H, 3.69; N, 13.57.

4-(2-(2-Methoxyethoxy)ethoxy)-2,6-bis[4-nitrophenyl-(thioureidocarbomoyl)]pyridine(4). Compound **4** was synthesized according to the above procedure using **11** (0.113 g, 1.03 mmol) and 4-nitrophenyl isothiocyanate (0.518 g, 2.88 mmol) in CH_3CN (20 mL). A pale yellow solid was obtained (0.784 g, 98%): mp 188−190 °C; HRMS (ES^+) calcd for $C_{26}H_{27}N_9O_9S_2Na$ $[M + Na]^+$ 696.1271, found 696.1240; δ_H (400 MHz, DMSO-d_6) 11.38−11.25 (2H, br m, NH_{amide}), 10.68−10.22 (4H, br m, NH_{urea}), 8.20 (4H, br s, Ar-*H*), 7.90 (4H, br s, Ar-*H*), 7.75 (2H, br s, H_{py}), 4.39 (2H, br s, CH_2,), 3.80 (2H, br s, CH_2), 3.61 (2H, m, CH_2), 3.46 (2H, m, CH_2), 3.24 (3H, s, OCH_3); δ_C (100 MHz, DMSO-d_6) 181.1 (C=S), 167.6 (q), 163.1 (C=O), 155.6 (q), 150.2 (q), 146.0 (q), 125.3 (CH), 124.0 (CH), 111.5 (CH), 71.7 (CH_2), 70.2 (CH_2), 68.9 (CH_2), 68.8 (CH_2), 58.5 (CH_3); IR ν_{max} (cm^{-1}) 3215, 2933, 1689, 1596, 1548, 1505, 1411, 1336, 1271, 1211, 1146, 1109, 1041, 996, 928, 878, 851, 775, 746, 698. Anal. Calcd for $C_{26}H_{27}N_9O_9S_2$: C, 46.35; H, 4.04; N, 18.71. Found: C, 46.19; H, 3.93; N, 18.72.

4,4′-(Ethoxyethoxy)ethyl)-2,6-bis-[4-trifluoromethylphenyl-(thioureidocarbomoyl)]pyridine] (5). Compound **5** was synthesized according to the above procedure using compound **12** (0.059 g, 0.114 mmol) and 4-trifluoromethylphenyl isothiocyanate (0.089 g, 0.447 mmol) and refluxed in CH_3CN (5 mL) for 20 h. The resulting precipitate was collected and dried by suction filtration, giving **5** as a white solid (0.101 g, 68%): mp >300 °C; HRMS (ES^+) calcd for $C_{52}H_{45}N_{14}O_8F_{12}S_4$ $[M + H]^+$ 1349.2236, found 1349.2284; δ_H (400 MHz, DMSO-d_6) 10.99 (4H, br s, NH_{amide}), 10.27 (4H, br s, NH_{urea}), 10.11 (4H, br s, NH_{urea}), 7.67−7.55 (20H, br m, Ar-*H*), 4.37−4.22 (4H, br m, CH_2), 3.82 (4H, br s, CH_2), 3.69 (4H, br s, CH_2); δ_C (100 MHz, DMSO-d_6) 180.9 (C=S), 167.1 (q), 162.7 (C=O), 149.1 (q), 142.6 (q), 125.4 (CH), 124.7 (CH), 124.8 (CH), 124.4 (CF_3, J_{13C9F} = 273.1 Hz), 110.6 (q), 70.3 (CH_2), 68.9 (CH_2), 68.3 (CH_2); IR ν_{max} (cm^{-1}) 3133, 2956, 1702 (C=O), 1602, 1548, 1480, 1416, 1324 (C=S), 1278, 1158, 1106, 1066, 1017, 997, 883, 838.

4,4′-(Ethoxyethoxy)ethyl)-2,6-bis[4-nitrophenyl-(thioureidocarbomoyl)]pyridine] (6). Compound **6** was synthesized according to the above procedure using compound **12** (0.106 g, 0.19 mmol) and 4-nitrophenyl isothiocyanate (0.142 g, 0.79 mmol) and refluxed in CH_3CN (5 mL) for 20 h. The precipitate was collected and dried by suction filtration, giving **6** as a pale yellow solid (0.215 g, 45%): mp 178−179 °C; HRMS (ES^+) calcd for $C_{48}H_{45}N_{18}O_{16}S_4$ [M + H] 1257.2144, found 1257.2189; δ_H (400 MHz, DMSO-d_6) 11.00 (4H, br s, NH_{amide}), 10.35 (4H, br s, NH_{urea}), 10.32 (4H, br s, NH_{urea}), 8.18−7.44 (20H, br m, Ar-*H*), 4.37−4.25 (4H, br m, CH_2), 3.83 (4H, br s, CH_2), 3.64 (4H, br s, CH_2); δ_C (100 MHz, DMSO-d_6) 181.0 (C=S), 167.7 (q), 163.2 (C=O), 149.5 (q), 145.5 (q), 143.8 (q), 124.7 (CH), 123.7 (CH), 123.6 (CH), 68.9 (CH_2), 69.4 (CH_2), 70.8 (CH_2); IR ν_{max} (cm^{-1}) 3215, 2933, 1689, 1596, 1548, 1505, 1411, 1336, 1271, 1211, 1146, 1109, 1041, 996, 928, 878, 851, 746, 698.

■ ASSOCIATED CONTENT

Ⓢ Supporting Information

General experimental description, synthesis and characterization of all intermediates, ^1H and ^{13}C NMR spectra of all intermediates and final products, and various figures and tables (see text for references). This material is available free of charge via the Internet at http://pubs.acs.org.

■ AUTHOR INFORMATION

Corresponding Author

*E-mail: gunnlaut@tcd.ie.

Notes

The authors declare no competing financial interest.

■ ACKNOWLEDGMENTS

We thank Science Foundation Ireland for an SFI RFP 2009 grant and HEA-PRTLI Cycle 3 and Cycle 4 (CSCB) and TCD for financial support. We thank Dr. John O'Brian for helping with NMR studies and Dr. Emma B. Veale and Dr. Jonathan A. Kitchen for helpful discussions.

■ REFERENCES

(1) (a) Gale, P. A; Gunnlaugsson, T. *Chem Soc. Rev.* **2010**, *39*, 3595. (b) Gale, P. A. *Chem Soc. Rev.* **2010**, *39*, 3746. (c) Steed, J. W. *Chem. Soc. Rev.* **2010**, *39*, 3686. (d) Hay, B. P. *Chem. Soc. Rev.* **2010**, *39*, 3700. (e) Li, A.-F.; Wang, J.-H.; Wang, F.; Jiang, Y.-B. *Chem. Soc. Rev.* **2010**, *39*, 3729. (f) Amendola, V.; Fabbrizzi, L.; Mosca, L. *Chem. Soc. Rev.* **2010**, *39*, 3889. (g) Duke, R. M.; Veale, E. B.; Pfeffer, F. M.; Kruger, P. E.; Gunnlaugsson, T. *Chem. Soc. Rev.* **2010**, *39*, 3936. (h) Veale, E. B.; Gunnlaugsson, T. *Annu. Rep. Prog. Chem., Sect. B: Org. Chem* **2010**, *106*, 376–406.

(2) (a) Wenzel, M.; Hiscock, J. R.; Gale, P. A. *Chem. Soc. Rev* **2012**, *41*, 480. (b) Gale, P. A.; Garcia-Garrido, S. E.; Garric, J. *Chem. Soc. Rev.* **2008**, *37*, 151. (c) Gunnlaugsson, T.; Glynn, M.; Tocci (née Hussey), G. M.; Kruger, P. E.; Pfeffer, F. M. *Coord. Chem. Rev.* **2006**, *250*, 3094. (d) Steed, J. W. *Chem. Commun.* **2006**, 2637. (e) Sessler, J. L.; Gale, P. A.; Cho, W. S. *Anion Receptor Chemistry*; Royal Society of Chemistry: Cambridge, UK, 2006.

(3) (a) Pradros, P.; Quesada, R. *Supramol. Chem.* **2008**, *20*, 201. (b) Filby, M. H.; Steed, J. W. *Coord. Chem. Rev.* **2006**, *250*, 3200. (c) Gale, P. A.; Quesada, R. *Coord. Chem. Rev.* **2006**, *250*, 3219. (d) Nguyen, B. T.; Anslyn, E. V. *Coord. Chem. Rev.* **2006**, *250*, 3118. (e) Gunnlaugsson, T.; Ali, H. D. P.; Glynn, M.; Kruger, P. E.; Hussey, G. M.; Pfeffer, F. M.; dos Santos, C. M. G.; Tierney, J. *J. Fluoresc.* **2005**, *15*, 287. (f) Martínez-Máñez, R.; Sancenón, F. *Chem. Rev.* **2003**, *103*, 4419.

(4) (a) Ghosh, K.; Saha, I.; Masanta, G.; Wang, E. B.; Parish, C. A. *Tetrahedron Lett.* **2010**, *51*, 343. (b) Ghosh, K.; Masanta, G.; Chattopadhyay, A. P. *Eur. J. Org. Chem.* **2009**, *26*, 4515. (c) Lowe, A. J.; Dyson, G. A.; Pfeffer, F. M. *Eur. J. Org. Chem.* **2008**, 1559. (d) Lowe, A. J.; Dyson, F. A.; Pfeffer, F. M. *Org. Biomol. Chem.* **2007**, *5*, 1343. Pfeffer, F. M.; Lim, K. F.; Sedgwick, K. J. *Org. Biomol. Chem.* **2007**, *5*, 1795. (e) Bates, G. W.; Triyanti; Light, M. E.; Albrecht, M.; Gale, P. A. *J. Org. Chem.* **2007**, *72*, 8921. (f) Liu, S.-Y.; Fang, L.; He, Y.-B.; Chan, W.-H.; Yeung, K.-T.; Cheng, Y.-K.; Yang, R.-H. *Org. Lett.* **2005**, *7*, 5825.

(5) (a) Veale, E. B.; Tocci, G. M.; Pfeffer, F. M.; Kruger, P. E.; Gunnlaugsson, T. *Org. Biomol. Chem.* **2009**, *7*, 3447. (b) dos Santos, C. M. G.; Gunnlaugsson, T. *Dalton Trans.* **2009**, 4712. (c) Duke, R. M.; Gunnlaugsson, T. *Tetrahedron Lett.* **2007**, *48*, 8043. (d) dos Santos, C. M. G.; McCabe, T.; Watson, G. W.; Kruger, P. E.; Gunnlaugsson, T. *J. Org. Chem.* **2008**, *73*, 9235. (e) dos Santos, C. M. G.; McCabe, T.; Gunnlaugsson, T. *Tetrahedron Lett.* **2007**, *48*, 3135. (f) Ali, H. D. P.; Kruger, P. E.; Gunnlaugsson, T. *New. J. Chem.* **2008**, *32*, 1153. (g) Gunnlaugsson, T.; Kruger, P. E.; Jensen, P.; Tierney, J.; Ali, H. D. P.; Hussey, G. M. *J. Org. Chem.* **2005**, *70*, 10875.

(6) (a) Duke, R. M.; Gunnlaugsson, T. *Tetrahedron Lett.* **2011**, *52*, 1503. (b) Pfeffer, F. M.; Kruger, P. E.; Gunnlaugsson, T. *Org. Biomol. Chem.* **2007**, *5*, 1894. (c) Pfeffer, F. M.; Buschgens, A. M.; Barnett, N. W.; Gunnlaugsson, T.; Kruger, P. E. *Tetrahedron Lett.* **2005**, *46*, 6579. (d) Pfeffer, F. M.; Gunnlaugsson, T.; Jensen, P.; Kruger, P. E. *Org. Lett.* **2005**, *7*, 5357. (e) Gunnlaugsson, T.; Davis, A. P.; O'Brien, J. E.; Glynn, M. *Org. Biomol. Chem.* **2005**, *3*, 48. (f) Gunnlaugsson, T; Davis, A. P.; Hussey, G. M.; Tierney, J; Glynn, M. *Org. Biomol. Chem.* **2004**, *2*, 1856. (g) Gunnlaugsson, T.; Kruger, P. E.; Jensen, P.; Pfeffer, F. M.; Hussey, G. M. *Tetrahedron Lett.* **2003**, *44*, 8909.

(7) Duke, R. M.; Gunnlaugsson, T. *Tetrahedron Lett.* **2010**, *51*, 5402.

(8) (a) Yang, R.; Liu, W.-X.; Shen, H.; Huang, H.-H.; Jiang, Y.-B. *J. Phys. Chem. B* **2008**, *112*, 5105. (b) Liu, W.-X.; Jiang, Y.-B. *Org. Biomol. Chem.* **2007**, *5*, 1771. (c) Evans, L. S.; Gale, P. A.; Light, M. E.; Quesada, R. *New J. Chem.* **2006**, *30*, 1019.

(9) Ali, H. D. P.; Quinn, S. J.; McCabe, T.; Kruger, P. E.; Gunnlaugsson, T. *New J. Chem.* **2009**, *33*, 793.

(10) (a) Quinlan, E.; Matthews, S. E.; Gunnlaugsson, T. *J. Org. Chem.* **2007**, *72*, 7497. (b) Quinlan, E.; Matthews, S. E.; Gunnlaugsson, T. *Tetrahedron Lett.* **2006**, *47*, 9333.

(11) Duke, R. M.; O'Brien, J. E.; McCabe, T.; Gunnlaugsson, T. *Org. Biomol. Chem.* **2008**, *6*, 4089.

(12) This cleft unit has also been used by: (a) Wei, L.-H.; He, Y.-B.; Wu, J.-L.; Meng, L.-Z.; Yang, X. *Supramol. Chem.* **2004**, *16*, 561. (b) Newton, A. *J. Am. Chem. Soc.* **1943**, *65*, 320.

(13) Vandevyver, C. D. B.; Chauvin, A. S.; Comby, S.; Bunzli, J. C. *Chem. Commun.* **2007**, 1716.

(14) Arnaud, A.; Belleney, J.; Boue, F.; Bouteiller, L.; Carrot, G.; Wintgens, V. *Angew. Chem., Int. Ed.* **2004**, *43*, 1718.

(15) Crystallographic data for **2** (CCDC 649247) M = 789.99, triclinic, a = 14.489(3) Å, b = 15.929(5) Å, c = 17.154(5) Å, α = 87.377(7)°, β = 68.142(6)°, γ = 81.774(8)°, V = 3636.5(17) Å^3, T = 123 K, space group P-1, Z = 4, μ(Mo Kα) = 0.381 mm^{-1}, 36636 reflections collected, 12 589 unique, (R_{int} = 0.0430), R = 0.0815, wR2 [$I > 2\sigma(I)$] = 0.2394. CCDC deposition no. 649247 for **6**.

(16) (a) Jiang, Q.-Q.; Darhkijav, B.; Liu, H.; Wang, F.; Li, Z.; Jiang, Y. B. *Chem. Asian J.* **2010**, *5*, 543. (b) Liu, W. X.; Yang, R.; Li, A. F.; Li, Z.; Gao, Y. F.; Luo., X. X.; Ruan, Y. B.; Jiang, Y. B. *Org. Biomol. Chem.* **2009**, *7*, 4021. (c) Li, Z.; Wu, F. Y.; Guo, L.; Li, A. F.; Jiang, Y. B. *J. Phys. Chem. B* **2008**, *112*, 7071. (d) Liu, W. X.; Jiang, Y. B. *J. Org. Chem.* **2008**, *73*, 1124.

(17) (a) Veale, E. B.; Gunnlaugsson. *J. Org. Chem.* **2008**, *73*, 8073. (b) dos Santos, C. M. G.; Gunnlaugsson, T. *Dalton Trans.* **2009**, 4712. (c) dos Santos, C. M. G.; Glynn, M.; McCabe, T.; De Melo, J. S. S.; Burrows, H. D.; Gunnlaugsson, T. *Supramol. Chem.* **2008**, *20*, 407.

(18) (a) Caltagirone, C.; Bates, G. W.; Gale, P. A.; Light, M. E. *Chem. Commun.* **2008**, 61. (b) Evans, L. S.; Gale, P. A.; Light, M. E.; Quesada, R. *Chem. Commun.* **2006**, 965.

(19) Cametti, M.; Rissanen, K. *Chem. Commun.* **2009**, 2809.

(20) Gale, P. A.; Hiscock, J. R.; Moore, S. J.; Caltagirone, C.; Hursthouse, M. B.; Light, M. E. *Chem.—Asian J.* **2010**, *5*, 555.

(21) (a) Gunnlaugsson, T.; Kruger, P. E.; Lee, T. C.; Parkesh, R.; Pfeffer, F. M.; Hussey, G. M. *Tetrahedron Lett.* **2003**, *44*, 6575. (b) Boiocchi, M.; Del Boca, L.; Gomez, D. E.; Fabbrizzi, L.; Licchelli, M.; Monzani., E. *J. Am. Chem. Soc.* **2004**, *50*, 16507.

(22) The AcO$^-$ was also best fitted to a 1:1 stoichiometric model, which resulted in a binding constant of log $K_{1:1}$ = 6.3 (±0.3). However, the fit was not ideal; therefore, this value was considered only an as estimation.

(23) No measurable changes were observed upon addition of group I ions to these solutions.

(24) We also carried out a spectrophotometric pH titration on **1** and **2** in this 1:1 mixture, the fitting of which gave rise to the determination of two pK_a values of 5.99 (±0.06) and 8.07 (±0.05) for **1**, while pK_a = 5.8(±0.07) and 7.6 (±0.06) was determined for **2**. Consequently, buffers such as MES and TRIS could not be used for these titrations. Such pH titrations usually have significant effect on the photophysical properties of such sensors, see: Gunnlaugsson, T.; Parker, D. *Chem. Commun.* **1998**, 511.

(25) In contrast, the addition of 10 equiv of TBAOH changed the pH from 7.3 to 11 for **1**.

(26) Sensors **5** and **6** also showed colorimetric changes similar to that observed in the absorption spectra of **1** and **2** for these anions in EtOH.

(27) It is worth pointing out that the addition of ATP to a solution of **6** in 1:1 MeOH–H_2O also showed colorimetric detection of this anion in a manner similar to that observed for **4**.